Azimuthal Asymmetries of the Charged Particle Densities in EAS in the Range of KASCADE-Grande

**O. Sima*, H. Rebel, C. Morariu*,
C. Manailescu*, and A. Haungs**

Institut für Kernphysik

*** Department of Physics,
  University of Bucharest, Romania**

Azimuthal asymmetries of the charged particle densities in EAS in the range of KASCADE-Grande

O. Sima*, H. Rebel, C. Morariu*, C. Manailescu*, and A. Haungs

Institut für Kernphysik

* Department of Physics, University of Bucharest, Romania

Abstract

The reconstruction of Extended Air Showers (EAS) observed by ground level particle detectors is based on the characteristics of observables like particle lateral density (PLD), arrival time signals etc. Lateral densities, inferred from detector data, are usually parameterized by applying various lateral distribution functions (LDF). The LDFs are used in turn for evaluating quantities like the total number of particles, the density at particular radial distances. Typical expressions for LDFs anticipate azimuthal symmetry of the density around the shower axis. The deviations of the particle lateral density from this assumption are smoothed out in the case of compact arrays like KASCADE, but not in the case of arrays like Grande, which only sample a smaller part of the azimuthal variation.

In this report we discuss the origin of the asymmetry: geometric, attenuation and geomagnetic effects. Geometric effects occur in the case of inclined showers, due to the fact that the observations are made in a plane different from the intrinsic shower plane. Hence the projection procedure from the observational plane to the relevant normal shower plane plays a significant role. Attenuation effects arise from the differences between the distances travelled by particles that reach the ground at the same radial coordinate but with various azimuthal positions in the case of inclined showers. The influence of the geomagnetic field distorts additionally the charged particle distributions in a way specific to the geomagnetic location. Based on dedicated CORSIKA simulations we have evaluated the magnitude of the effects. Focused to geometric and attenuation effects, procedures for minimizing the effects of the azimuthal asymmetry of lateral density in the intrinsic shower plane were developed. The consequences of the reconstruction of the charge particle sizes determined with the Grande array are also discussed and a procedure for practical application of restoring the azimuthal symmetry is outlined.

Zusammenfassung

Azimutale Asymmetrien der lateralen Dichteverteilung geladener Teilchen von ausgedehnten Luftschauern im Bereich von KASCADE-Grande

Die Rekonstruktion von ausgedehnten Luftschauern (EAS), die am Boden mit Teilchendetektoren beobachtet werden, basiert auf den Charakteristika von Observablen wie der lateralen Verteilung der Teilchendichte, den Verteilungen der Ankunftszeiten etc. Die lateralen Dichteverteilungen, die aus den Detektordaten rekonstruiert werden, werden üblicherweise mit verschiedenen funktionalen Formen (LDF) parametrisiert. Die Verteilungen dienen dann dazu, um die Schauer durch die Gesamtzahl der Teilchen und die Dichte an bestimmten radialen Abständen von der Schauerachse zu kennzeichnen. Die funktionalen Ausdrücke für die LDF setzen in der Regel eine azimutale Symmetrie der Teilchendichte voraus. Experimentelle Abweichungen von dieser Annahme werden bei kompakten Detektorarrays teilweise ausgewaschen, allerdings nicht in dem Falle, wenn nur ein beschränkter Teil der Detektoren die gesamte azimutale Verteilung überdeckt, wie dies oft bei KASCADE Grande der Fall ist.

In diesem Bericht diskutieren wir die Gründe für azimutale Variationen und Asymmetrien der lateralen Dichte von EAS Teilchen: rein geometrische Effekte beim Einfall schräger Schauer, Effekte der unterschiedlichen Abschwächung der Teilchendichte und der Einfluss des geomagnetischen Feldes. Geometrische Effekte im Falle schräg einfallender Schauer rühren von der Tatsache her, das die experimentellen Beobachtungen in einer Ebene gemacht werden, die verschieden ist von der intrinsischen Schauerebene senkrecht zur Schauerachse. Daher spielt das Verfahren der Projektion von der Beobachtungsebene in die relevante Schauerebene eine signifikante Rolle. Abschwächungs - Effekte haben ihren Grund in den unterschiedlichen Weglängen der Teilchen, wenn sie die Beobachtungsebene

erreichen beim gleichen radialen Abstand von dem Schauerkern, doch mit verschiedenen azimutalen Positionen. Darüber hinaus verbiegt auch das geomagnetische Feld die Teilchenbahnen, abhängig von der EAS -Einfallsrichtung relativ zur Richtung des magnetischen Erdfeldes.

Auf der Basis von EAS -Simulationen mit dem Monte Carlo Programm CORSIKA, wird die Größe der Effekte untersucht. Wir konzentrieren unsere Studien in diesem Bericht auf die geometrischen und die Abschwächungs-Effekte und entwickeln Verfahren, diese Effekte bei der Rekonstruktion der Schauerobservablen zu minimalisieren. An einem Beispiel für die Lateralverteilung, die mit KASCADE Grande beobachtet wird, wird das Verfahren, die azimutale Symmetrie wiederherzustellen, demonstriert.

Contents

1   Introduction

The analysis of extensive air showers (EAS) generated by interactions of high energy particles entering from the outer space the Earths atmosphere is the practised standard method of investigations of the energy spectrum and mass composition of primary cosmic rays. Correlated and interwoven with these questions is the study of the characteristics of the interactions of the incident primary particles at energies beyond the energy range accessible by artificial accelerators [1].

A crucial EAS observable is the lateral distribution of the EAS particles (of various different EAS components) in a plane perpendicular to the shower axis at the observation level. The particle density distributions (PLD) and their correlations with various EAS components carry important information about the primary particles and are used to determine the energy and mass of the primary. The first step on this way is to deduce the density of particles from the registered detector signals, e.g. in case of scintillation detectors from the energy deposits in the scintillators. Already this step needs careful consideration since the energy deposit depends on the direction of particle incidence [2]. Subsequently the reconstructed particle densities are usually parameterised by adequate forms (LDF) adjusted to the simulated or experimental data deduced from measurements. There are various LDFs, e.g. the well known NKG form [3] and various others which have been studied by simulations [4] and are proven to describe the data in generally fairly well for EAS of zenith angles $< 40°$. When analysing experimental air shower observations or shower simulation output, it is usually assumed that the footprint of an extensive air shower in the observational plane on ground has elliptical symmetry, centred to the shower axis, and that a simple transformation into a plane perpendicular to the shower axis will restore circular symmetry. Therefore the lateral distribution functions (LDF) are assumed to be dependent only from the radial distance from the shower axis.

In fact for *inclined showers* this is clearly not the case. The cascade continues to develop when the shower hits the ground; particles which strike the ground first represent an earlier stage than those which arrive later and have experienced additional attenuation. Additionally, even for near vertical showers, there are asymmetries due to the effects of the geomagnetic field. This is in particular the case for muons, which travel large distances through the atmosphere with minor interaction. Thus the assumption of circular symmetry may lead to systematic errors in the core location, arrival times (angle of incidence) and in the deduced shower parameters. In addition to geometric effects [5,6,7] arising from the projection from the observational shower plane onto the shower plane normal to the axis and the effects originating from the attenuation [6,7,8] of the densities due to different path lengths travelled by particles at different sides of inclined showers, the Earth s magnetic field distorts also the shape of the lateral distributions. The intriguing effects arising from the geomagnetic field on the lateral distributions have been regarded in various papers [9-11]. The geomagnetic influence is not only efficient at very large zenith angles with long path lengths of the particles in the atmosphere, it depends explicitly on the geomagnetic angle i.e. the relative angle of the direction of shower incidence and the geomagnetic vector, that means on the *azimuthal* angle of shower incidence [10,11].

In the present report we communicate on studies of the asymmetries on basis of shower simulations by CORSIKA [12], vers.6.01, with the motivation to develop feasible methods to restore (at least approximately) the radial symmetry of the lateral distribution in the normal plane. Here we mainly focus to deviations from the azimuthal symmetry, which arise from an interplay of geometrical features with the attenuation of the shower intensity in the atmosphere. They are of particular interest for a detector configuration like KASCADE-Grande [13], which in general does not allow a complete integration of the lateral density function around the shower core. They are important at large distances and for the reconstruction of the muon density from the KASCADE array, which is located in the North -

East corner of the Grande area. A feasible procedure for restoring the circular symmetry for practical use is outlined.

2 Basic Origin of Asymmetries

First, for sake of simplicity we assume that the shower is arriving from infinity as a cylinder. The intersection of such a cylinder with the horizontal plane is elliptically shaped for inclined showers, with elliptical iso-density contours. When ground array data are analyzed with assuming cylindrical symmetry, various geometrical asymmetries arise i.e. an azimuthal dependence of the particle density, independent of any additional attenuation differences on different sites of the shower.

More realistically the shower disk does not move undisturbed through the atmosphere. It continues to develop and get attenuated after the shower maximum. That means the distances of iso-density contours from the shower axis shrink. This is the scenario of an inverted cone. In this case the contours of equal density in the horizontal plane, where our detectors are located, are eccentric ellipses, dividing the shower footprint in two sides: the "fast" side where the particles arrive earlier and the density is higher, and the "late" side, where the particles have travelled a longer distance and appear with reduced density, also due to increased decay probability.

When these ellipses are projected into a plane perpendicular to the conical axis, the eccentricity gets reduced, but it is not eliminated. This feature is the object of our attention. In other words, when studying the lateral density at a fixed distance from the shower axis there exist azimuthal variations.
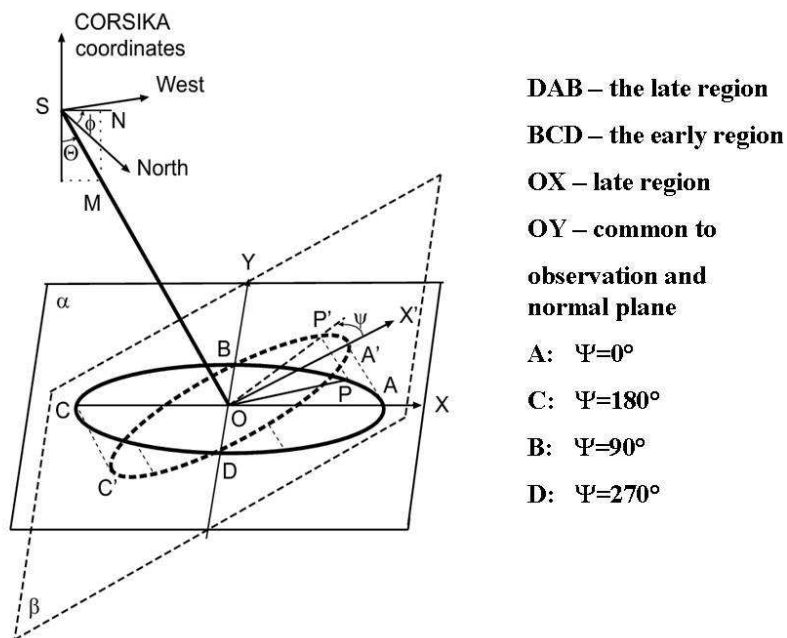

Figure 1: *The EAS - intrinsic coordinate system*

For detailed considerations it is convenient to use the *intrinsic* EAS coordinate system of the cascade, as shown in Fig.1: the zone BCD stands for the prompt ("fast") part of the shower, while the zone BAD stands for the "late" part. Due to the geometric effect it is expected, that at the same distance r from the shower core, for $\Psi = 0°$ and $\Psi = 180°$ the particle density is larger than for $\Psi = 90°$ and $\Psi = 270°$. As *geometrical effect* we call the feature (Fig.2):
The density at the radial distance r from the shower centre in the observation plane corresponds to the density at the radial distance $r \cdot \cos(\Theta)$ in the normal plane at $\Psi_{norm} = 0°$

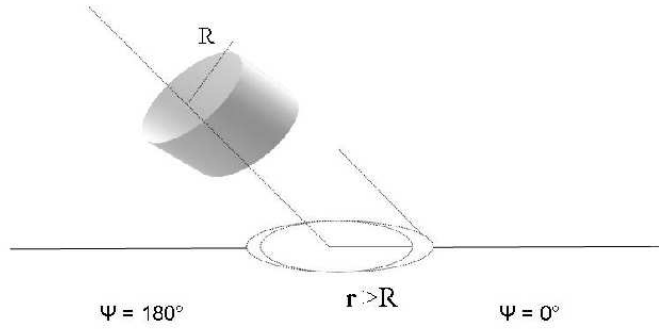*and Ψ_{norm} = 180°, but that of the radius r (= R) for Ψ = 90° and Ψ = 270°.*
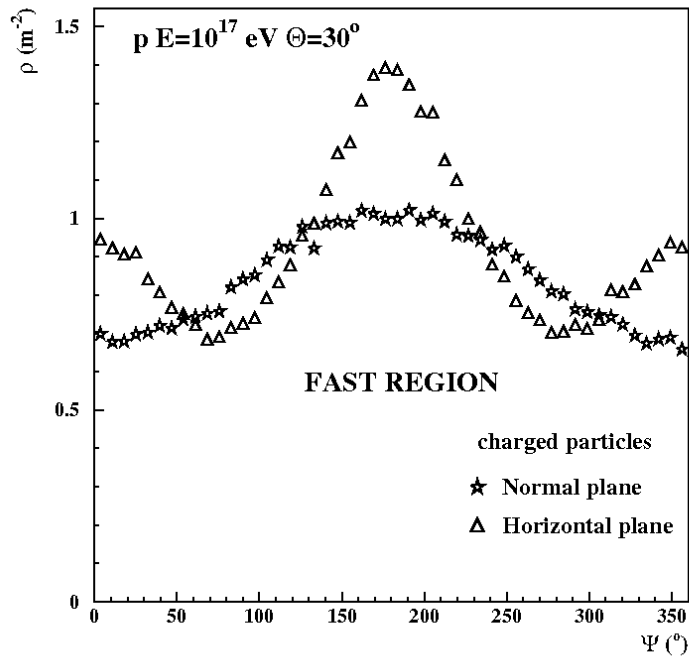

Figure 2: *Illustration of the geometrical effect*

Figure 3: *Azimuthal variation of the lateral distribution of charged EAS particles (r=450-500 m)*

Fig. 3 displays the result of a realistic simulation of the azimuthal variation of the lateral distribution of a particular shower, incident with θ = 30°. It exhibits all typical features:

- The dominant contribution for the asymmetry between the "fast" region (Ψ = 180°) and the "late" region (Ψ = 0°) originates from the additional attenuation on the late

side. For inclined showers hitting the observational plane, charged particles arriving first do experience less attenuation as the particles arriving later have travelled larger distances, increasingly with the impact radius r.

- The enhancement at $\Psi = 0°$ in the observation plane is due to the geometric effect.

- The azimuthal asymmetry is also evident when projecting the observed particle densities (or energy deposits in the detectors) to the more relevant intrinsic shower plane, normal to the axis of the shower.

For the present simulations the influence of the geomagnetic field on the lateral distribution has been ignored. In fact it leads a further asymmetry effect. But it appears to be less obvious, as long all charged particles are considered and as long there is no differentiation between positive and negative muons. For very inclined showers where the charge particle component is dominated by muons, there appears a double structured core with shifts of the core position [14]. In the following we focus our studies to the global origin of the asymmetries.

3   Different projection methods onto the normal shower plane

a. Procedures

For mapping the particle densities in the normal plane on the basis of particle densities observed in the observation plane, the common standard procedure projects the densities in the normal plane by projecting the particle impact point from the observation level onto the normal plane in direction of the shower axis. This method (1), though the only practical one for experimental data, implies some inaccuracies. Due to the geometric effect it introduces an artificial dependence of the lateral distributions from the azimuth measured in the normal plane with respect to the shower axis.

More rigorous would be (method 2) the reconstruction of the densities in the normal plane by projecting each impact point along the particle trajectory. If the particles would not interact (by absorption and scattering) in the atmosphere in between the horizontal and the normal plane, it would be a completely correct method, removing the asymmetries. However it requires the knowledge of the momentum vector of the particles (which is available by the CORSIKA results, but not for experimental data). Fig. 4, which will be discussed below, indicates the features.

Alternatively (method 3) the densities in the normal plane may be deduced by a two-steps procedure. The first step assumes that the global arrival time (relative to the shower center) is known. Additionally assuming that the particle has been produced on the shower axis and does not experience substantial scattering on its way to the observation level, the particle production locus can be computed by triangulation. Under these conditions the intersection of the trajectory starting from the production point and ending in the observation level with the normal plane is obtained. This procedure is useful for higher-energy muons.
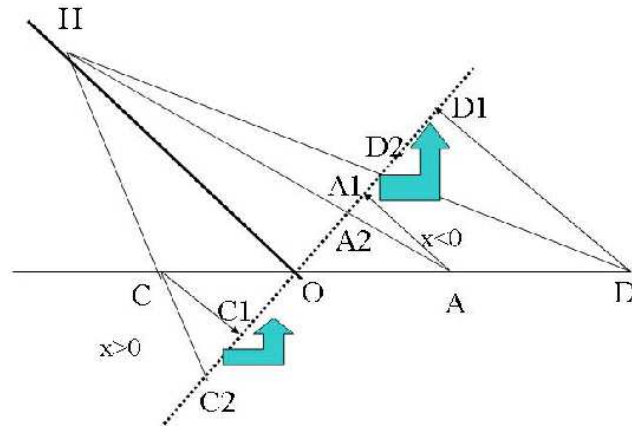

Figure 4: *Effects of different projection procedures*

b. Details of the distortions introduced by the orthogonal projection procedure

Considering a shower that comes from a finite distance and assuming that the particles do not suffer any interaction between the observation plane and the normal plane, it is possible to deduce some more detailed characteristics of the densities resulting from the orthogonal procedure.

Fig.4 reveals that the density in the early region reconstructed in OC1 is overestimated; the particles that are reconstructed in the radial range OC1 in fact would have been correctly reconstructed in a broader range, OC2, resulting in a smaller density in OC1. Contrary, the density in the late region in the radial range OA1 is underestimated, because the particles that are reconstructed in the range OA1 in fact would hit the normal plane in OA2. But it is not true that the density is overestimated over the complete early region and underestimated over the complete late region In fact at large radial distances the situation is reversed.

Consider for example the particles reconstructed in the radial range A1D1 in the late region. Actually they would have hit the normal plane in the A2D2 radial range. Clearly the mean density per solid angle in the region A2D2 is higher than the mean density per solid angle in the region A1D1; but it can be geometrically demonstrated that the solid angle delimited by A2HD2 is smaller than the solid angle delimited by A1HD1. So the total number of particles reconstructed by the orthogonal projection on A1D1 (which is in fact the number of particles from the solid angle delimited by A2HD2) is higher or lower than the true number of particles that would have hit the range A1D1 depending on the balance between the increased mean density per solid angle in A2HD2 and the smaller solid angle A2HD2 in comparison with the corresponding values in the solid angle A1HD1. It can be expected that in the case of small radial ranges the decrease in the density (which is very fast) to be the dominant factor, and consequently the density to be underestimated, while at larger distances, where the density slope is smaller, the increase in the solid angle to be the dominating factor, and consequently the density should be overestimated by the orthogonal projection method.

A similar consideration for the case of the early region leads to the conclusion that at small radial ranges the orthogonal projection method should overestimate the density, while at larger distances from the axis it should underestimate the density. Due to the fact that the angles subtended by equal radial ranges are higher in the early region than in the late region, it is expected that the distortions are more significant in the early region, at least not very far from the axis.

From geometrical considerations it is obvious that the distortion of the density is smaller if the shower starts very high in altitude and it is larger in the opposite case. Due to the fact that the muons are generally produced at higher altitude than the electrons or photons that are measured at the same radial distance, it is expected that the effect for distortion of the density is smaller for muons than for electrons or photons. It is also expected that the distortions increase with the zenith angle of EAS incidence.

At what radial range the small - radius dependence is turned to the large - radius dependence depends on the particle and on the energy. The solid angle arguments let expect the distortion to be smaller for showers starting at higher altitude, but the other quantity, the slope of the density, depends on the nature of the secondary particle and on the type, energy and incidence angle of the primary.

If the interaction of the particles in the atmosphere between the observation and the normal planes would be negligible, the second method of projection (along the particle momentum) would give correct results. If attenuation is present it affects simultaneously, in the same way, the results obtained both with the orthogonal projection and with the projection along the particle momentum (it affects the particles that hit the observation level, i.e. the input of both reconstruction procedures). Therefore the relative behaviour of the density reconstructed with Method 1 and with Method 2 should be practically independent of the attenuation. For example, if by Method 1 the density would be overestimated with

respect to Method 2 (which would give the correct result) in the absence of attenuation, then it should give densities higher than the densities given by Method 2 also in the presence of attenuation. So the geometric distortion presented above can be observed in the presence of attenuation by comparing the densities reconstructed with Method 1 with the densities reconstructed with Method 2.
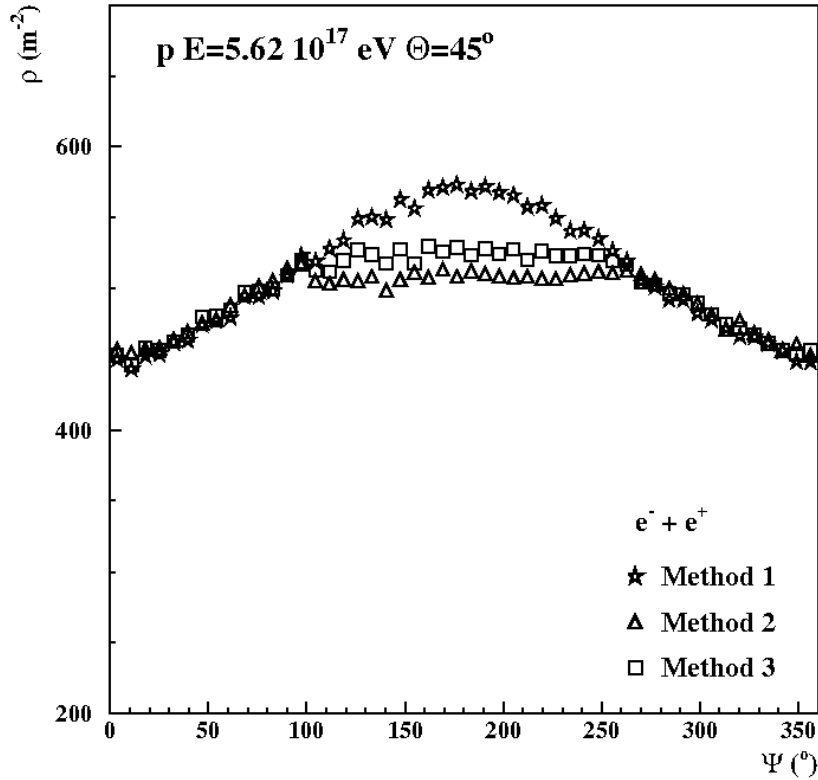

Figure 5: *The electron density in the radial range of 20-30 m displaying the overestimation of the density in the early region (around $\Psi = 180°$) by the orthogonal projection*

Figs. 5 - 10 display the comparison between the densities reconstructed with the 3 methods, both with the small - radius behaviour (Figs. 5-7), where the orthogonal method overestimates the density in the early region, and the large - radius behaviour (Fig. 9). The muon density is practically not much affected by geometrical distortions (see Fig. 8 and Fig. 10); the additional attenuation is seen on all the figures, except in Fig.8 (for muons close to the core). Fig.8 is affected by low statistical accuracy since only two simulated EAS were available for the case of the highest energies.

The geometric distortion, introduced by the orthogonal projection, especially in the region of small radii has the consequence to mimic a high attenuation in this radial range so far the azimuthal behaviour of the density is attributed to attenuation effects. An equivalent attenuation coefficient (see next chapter) which includes the geometrical distortion by the projection method will decrease with increasing radius in the EAS plane, but for radial distances beyond 200 m it will have a less pronounced variation with radius.
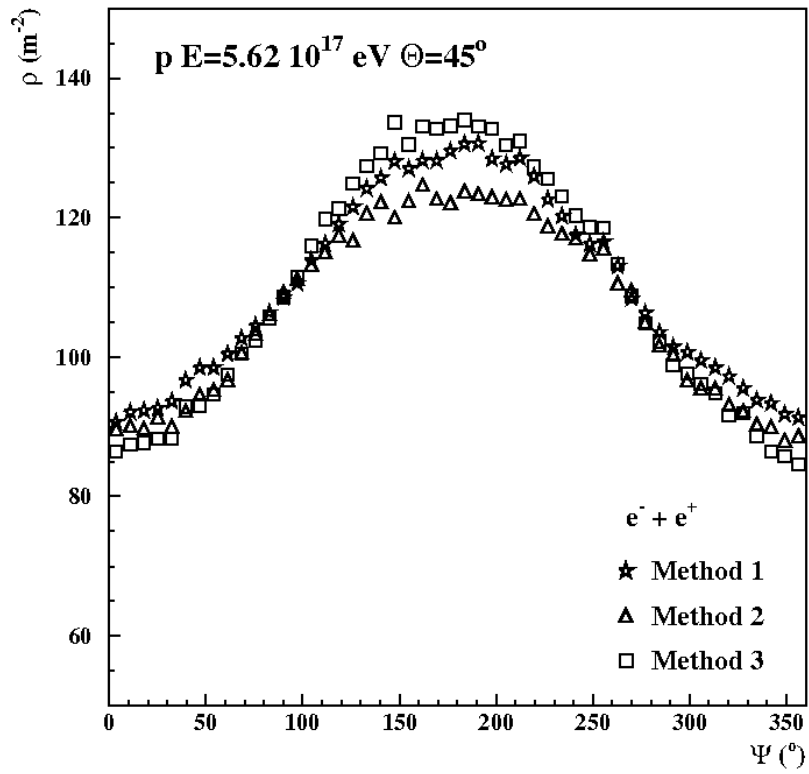
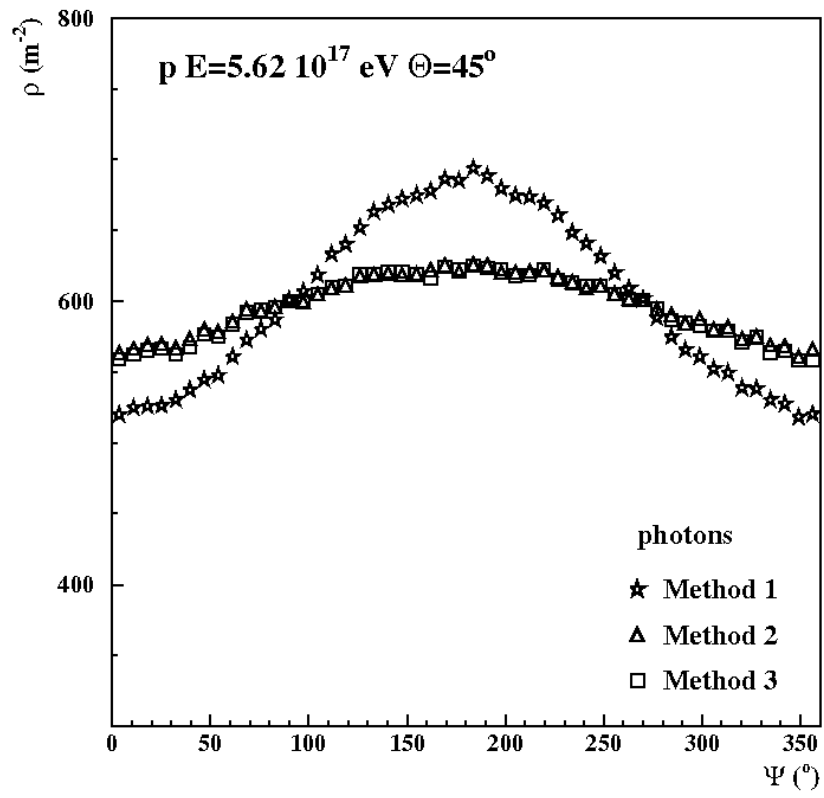Figure 6: *The electron density at 50-60 m distance from the EAS axis*

Figure 7: *The photon density at 50-60 m distance from the EAS axis*
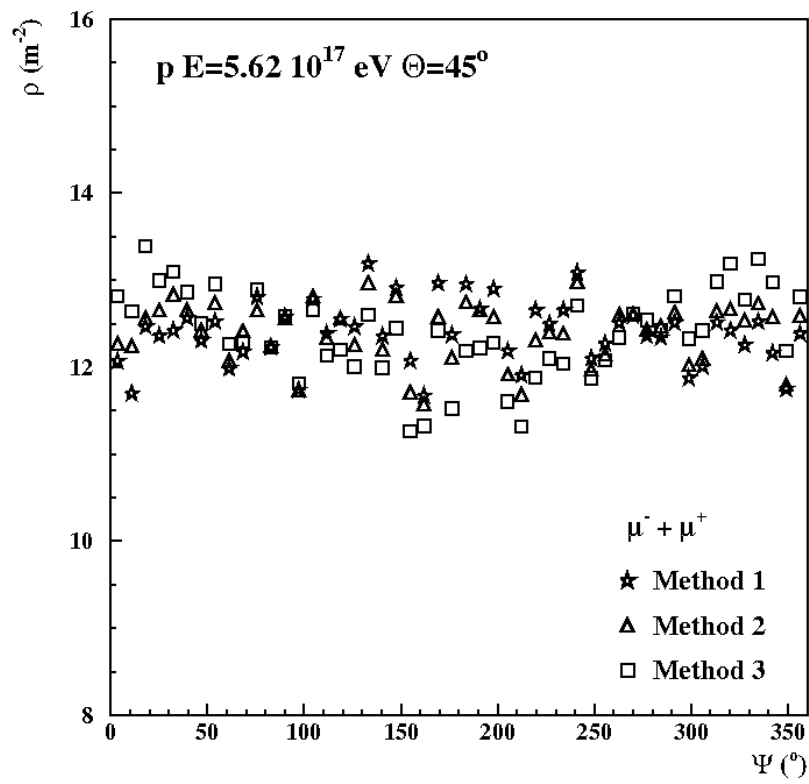
Figure 8: *The muon density in the radial range of 50-60 m distance from the shower axis*
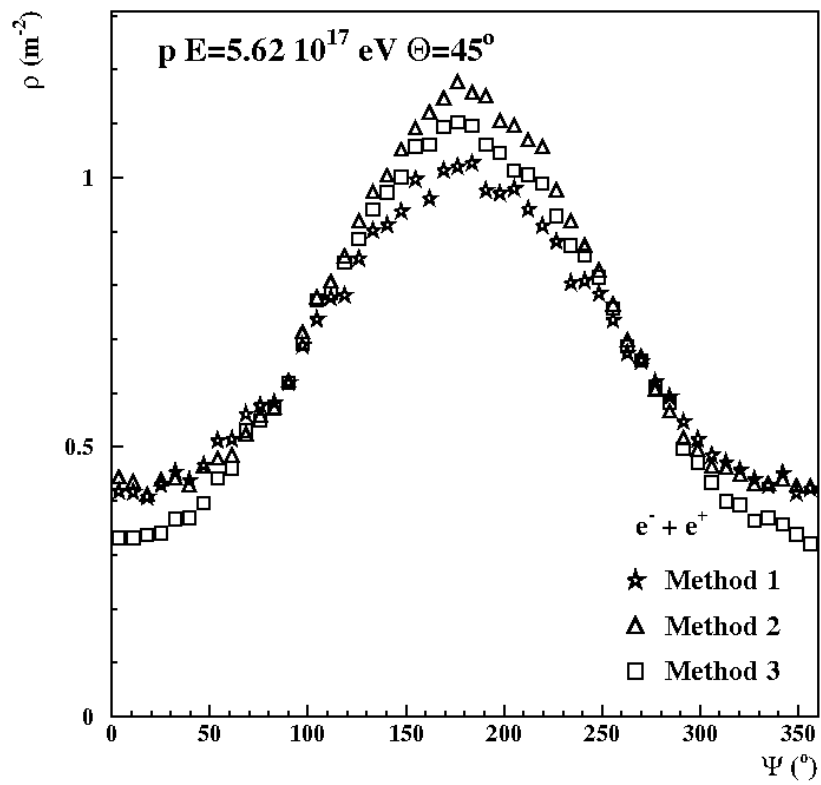
Figure 9: *The electron density at 450   500 m distance from the shower axis: At large distances the orthogonal method underestimates the density in the early region*
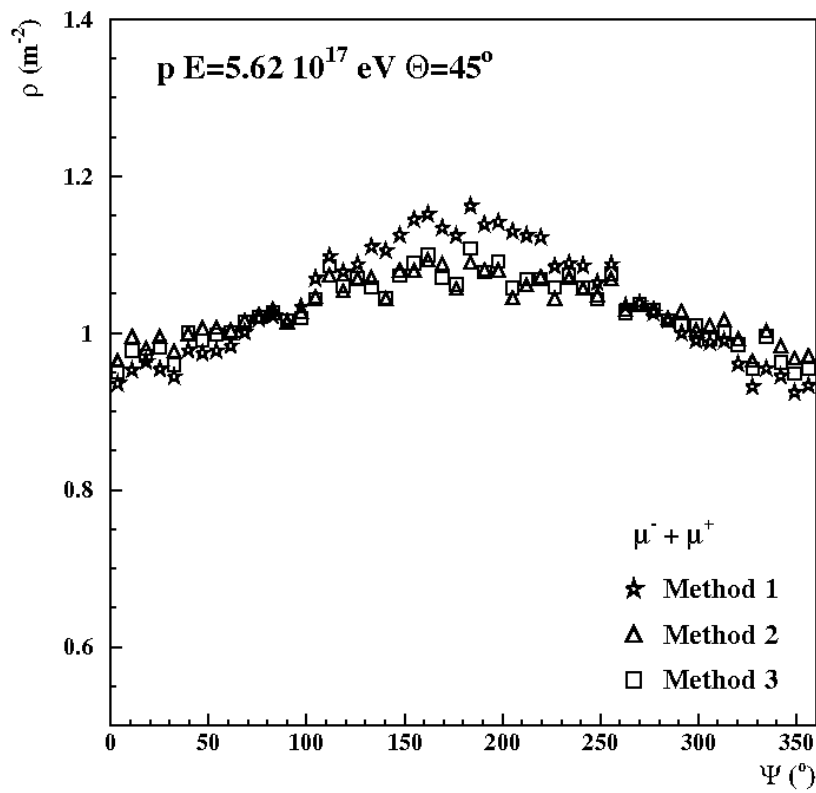
Figure 10: *The muon density in the radial range 450-500 m distance from the EAS axis*

4   Attenuation

In the step mapping the particle impacts to the normal plane no interaction is assumed in the space between the normal plane and the horizontal plane. Hence the results of the projection show clearly the early late region asymmetries, as detailed by the examples of the preceding Figs. 5-10.

For the correction we apply a basically simple method along the following considerations:

- For the two azimuth angles 90° and 270° the reconstructed density in the normal plane is correct. As the true density in the normal plane should exhibit circular symmetry, the density at r_{norm} at any angle in the normal plane should be equal to the density at the same r_{norm} evaluated at 90° or 270°. For all the other points, attenuation and scattering of the particles observed in the observational plane should affect the density in the normal plane.

- We define as reference ρ_{ref} the density in the normal plane at x=0 (this is the case for $\Psi_{norm} = 90°$ or 270°) while for x≠0 an exponential attenuation is adopted, tacitly assuming that the orthogonal projection would be approximately correct for specifying x

$$\rho_i(r_{norm}, \Psi_{norm}) = \rho_{ref,i}(r_{norm}) \cdot \exp[-\lambda_i \cdot x(r_{norm}, \Psi_{norm})]) .$$

Various procedures have been applied for specifying the value of $\rho_{ref,i}(r_{norm})$ and deriving the exponential factor $f_i = \exp[-\lambda_i \cdot x(r_{norm}, \Psi_{norm})])$. The determination of the correction factors was done by fitting the following expressions:

$$\ln[\rho_i(r_{norm}, \Psi_{norm})/\rho_{ref,i}(r_{norm})] = -\lambda_i \cdot x$$

or when $-\lambda_i \cdot x \ll 1$

$$\rho_i(r_{norm}, \Psi_{norm})/\rho_{ref,i}(r_{norm}) = 1 - \lambda_i \cdot x$$

For a given zenith angle Θ of EAS incidence, the distance x is related to r_{norm} and the azimuth Ψ_{norm} by

$$x = r \cdot \cos \Psi \cdot \tan \Theta$$

(omitting furtheron the indication of the normal plane).

It should be explicitly noted that x depends on the product of r and $\cos \Psi$, so that different combinations (r, $\cos \Psi$) do contribute to a particular x-value.

There is approximately a *linear* dependence between the logarithm of the normalised density and the distance x, with a slope being the attenuation coefficient. The determination of the correction factors λ_i as done by fitting the above expressions for many simulated showers of various *primary energies, zenith angles of incidence and different shower particles*. Fig. 11 displays an example of determining the attenuation coefficient for the electron component averaged over the considered x-range, each x bin being an average over various azimuth angles and distances from the EAS core. For example, for small x-values small r values contribute as well as larger r-values from the region of the intersection of the normal plane with the horizontal plane (even far from the shower core).
Detailed studies reveal that the attenuation factors λ_i mainly depend on the zenith angle and less on energy [15].

Above we have indicated that there is also a noticeable dependence of the attenuation factors λ_i of the radial distance, induced by distortions by using the orthogonal projection method: The attenuation coefficient will decrease with increasing radius in the EAS plane,
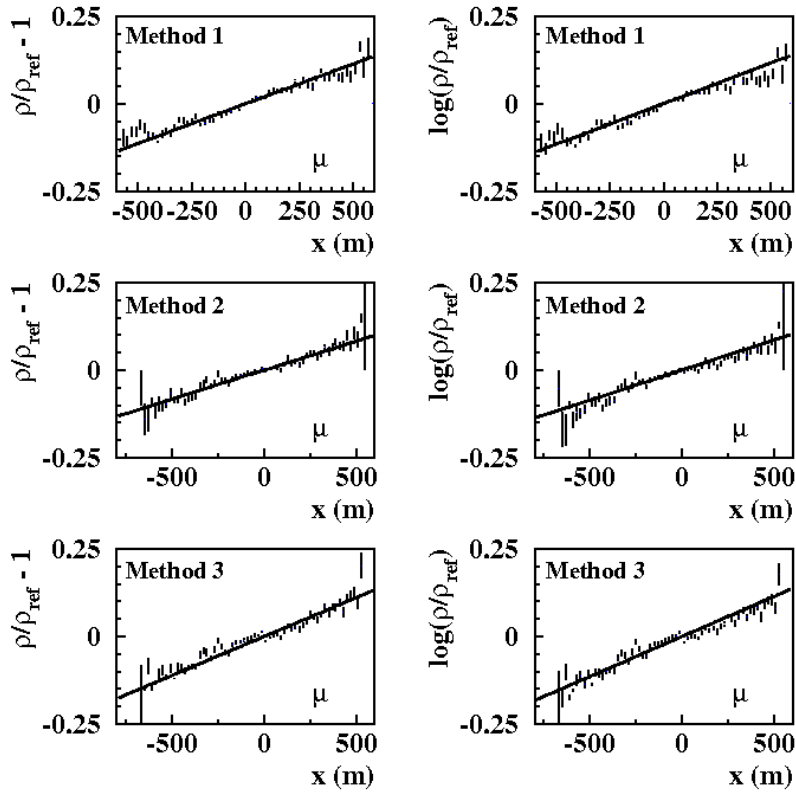
Figure 11: *Linear fits of the normalised density*

while it appears increased at low radii for the early shower side. In order to display this feature the attenuation coefficients have been determined by fixing the radial range and fitting the normalized density as a function of x (through the dependence of x on cos Ψ). The results are shown in Figs.12 and 13, based on the projection by method 1. One reason for the decrease of the attenuation with the radial distance is indeed the imperfection of the orthogonal projection. As we have outlined above (see e.g. Fig. 4) the density close to the core is artificially increased, while the density in the late region appears to be decreased. This leads to an enhanced apparent attenuation at low radii. The situation is reversed at larger radii. Additionally there might be also a gradual change of the energy per particle with the distance from the core, which plays a role.

The dashed curves in Figs. 12 and 13 indicate a fit by a (A+B/(C+r)) parametrization.

Fig. 14 shows, how the procedures restore the azimuthal symmetry of the electron component, for the particular example of the lateral distribution of the electron component, observed at a distance from the shower axis of 450-500 m.
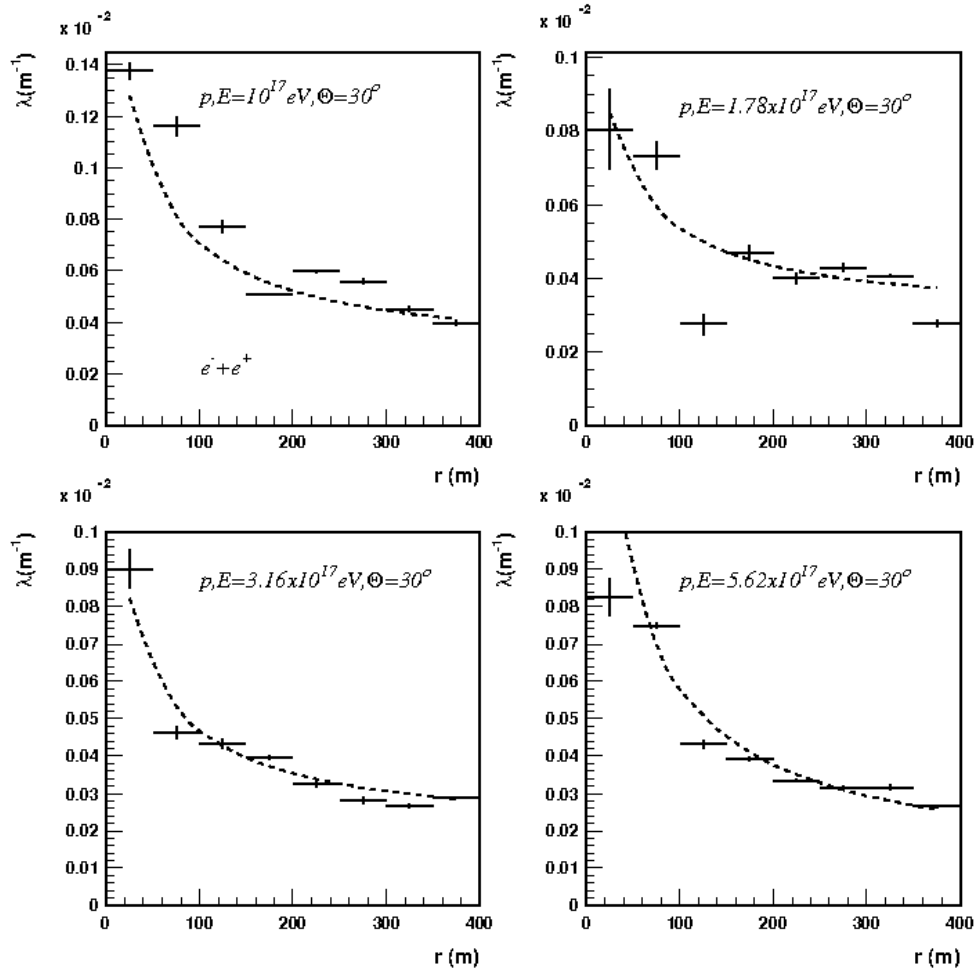
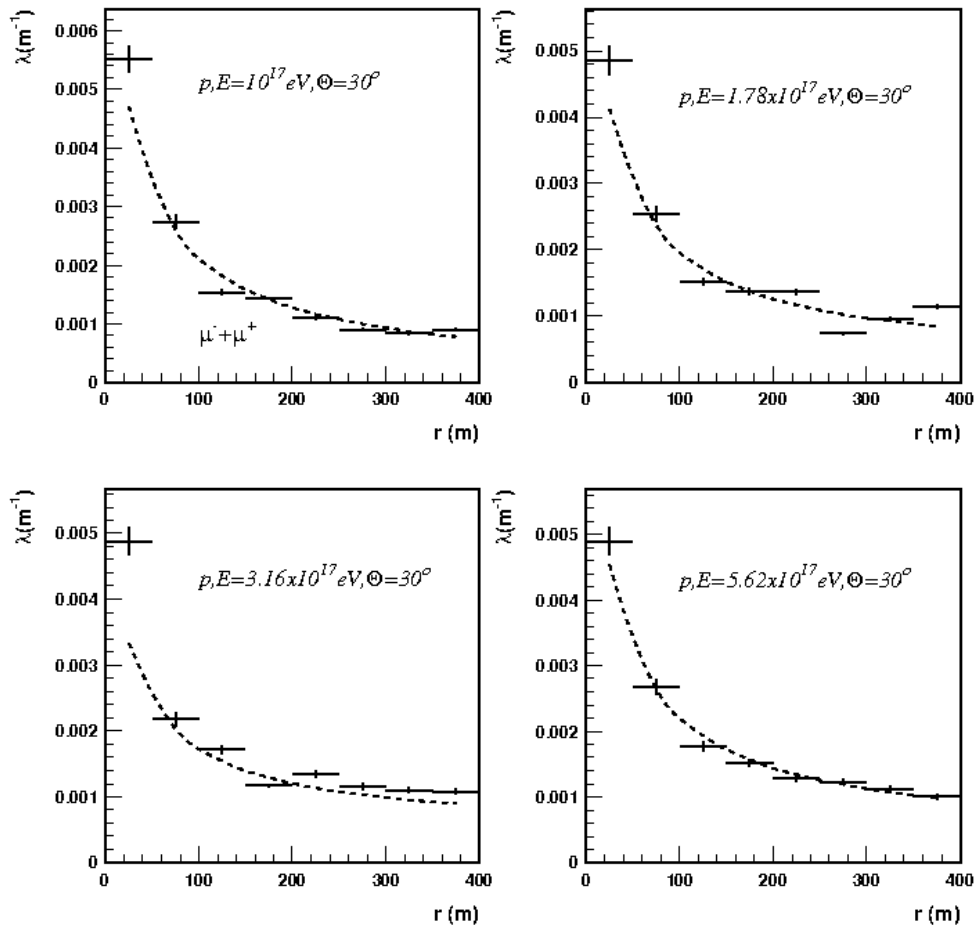Figure 12: *Attenuation coefficient dependence of the radial distance r: electron component*

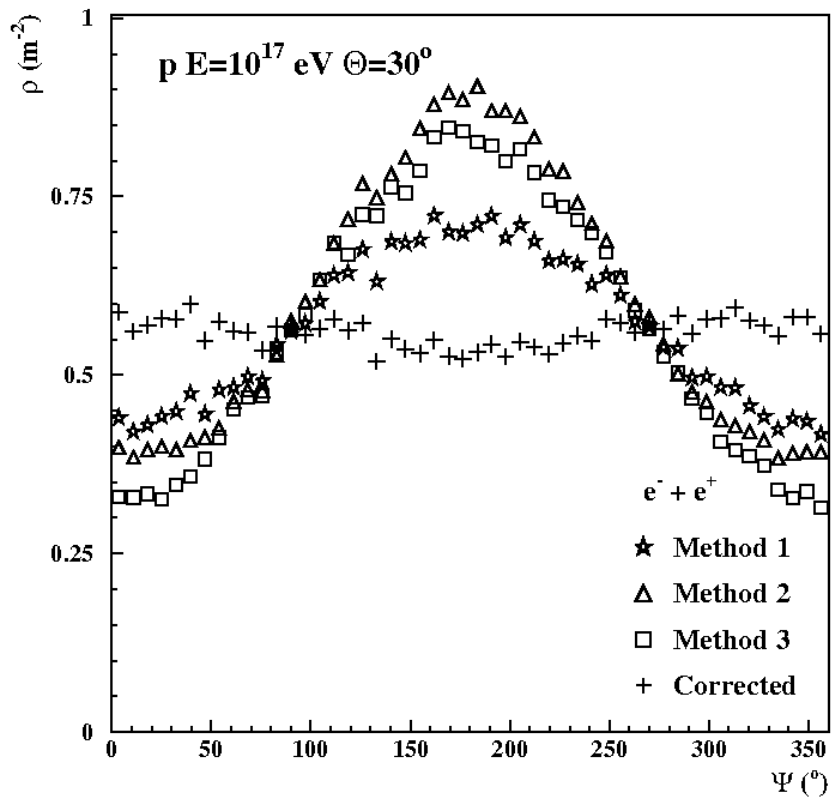Figure 13: *Attenuation coefficient dependence of the radial distance r: muon component*

Figure 14: *Application of the asymmetry correction to the azimuthal distribution (r =450-500 m)*

5 Application example: Determination of the charged particle density distribution.

Obviously there are some difficulties of a direct observation of the attenuation effects in experimental data. In a single shower seldom a sufficient number of detectors in the same radial bin is hit with enabling the observation of the azimuthal dependence in the same radial bin. In a set of showers the fluctuations from shower to shower are generally high and also in this case the number of detectors in the same radial and azimuthal bin is limited (even if several detectors would be located in the same radial bin with *different* azimuthal coordinates), so that the decrease of the fluctuations due to averaging is not very efficient. Furthermore, due to the steep radial dependence of the lateral distribution, uncertainties of the core position have an appreciable effect on the density. That feature may obscure the azimuthal dependence. Nevertheless it is important to stress that the above effects are of a *statistical* nature, while the attenuation effects result in a *systematic* dependence, and neglecting them would lead to biased results.
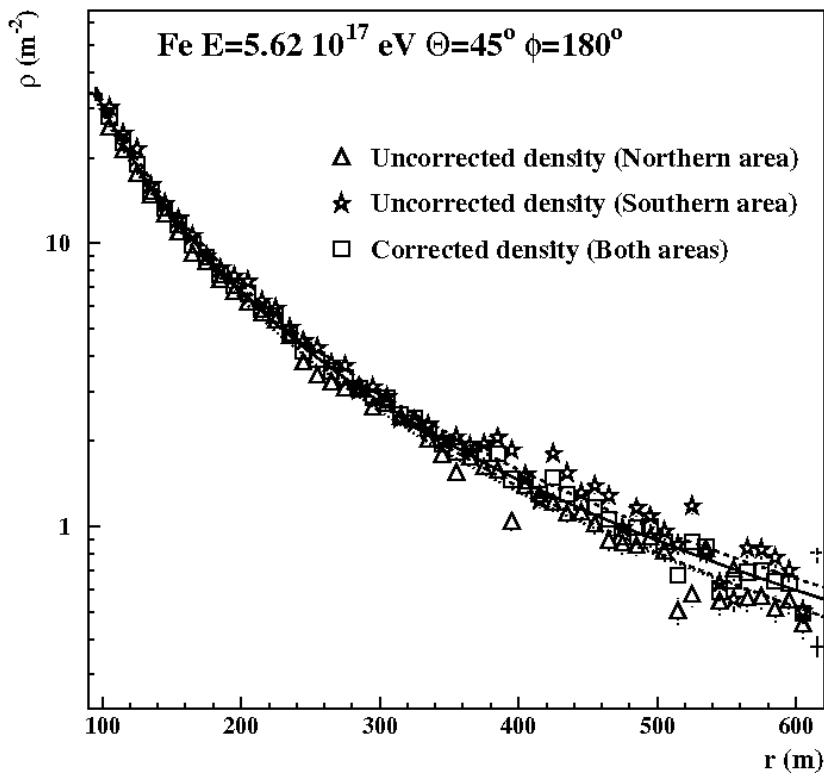

Figure 15: *Comparison of the uncorrected lateral density distribution of charged particles for different core areas (Fe). Linsley fits of the uncorrected density for showers with the core in the northern area (dots) and southern area (dashes) respectively, and of the corrected density (full line)*

In the following we present two examples illustrating the application of the attenuation corrections in simulated data that realistically mimic the experimental data. We consider an iron induced shower of the primary energy $E = 5.62 \cdot 10^{17}$ eV ($\theta = 45°$), incident from North, and a proton induced shower with $E = 3.16 \cdot 10^{17}$ eV ($\theta = 45°$) coming also from North. In order to suppress the effects of the magnetic field, the showers were simulated
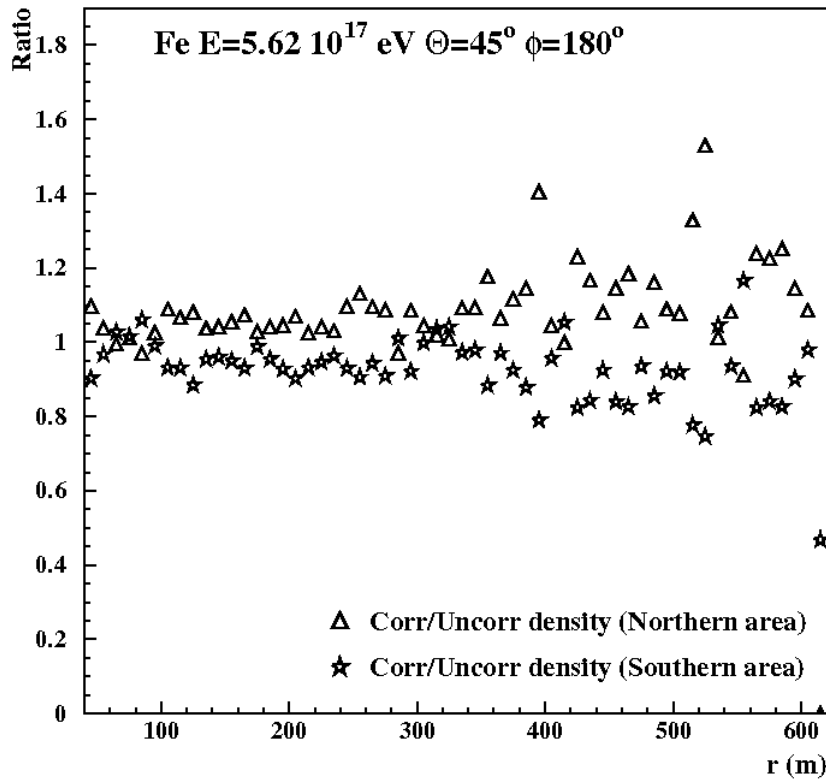
Figure 16: *The ratios of the corrected to the uncorrected densities (iron induced EAS)*

using CORSIKA [12] in the absence of the magnetic field. When in the above cases the cores are located in the northern part of the KASCADE-Grande area, most of the hit detectors will be situated in the late region of the shower. On the other side, when the shower cores are located in the southern part of the KASCADE-Grande area, then most of the hit detectors are situated in the early region of the showers. Consequently, in the absence of the attenuation corrections we expect higher particle densities reconstructed in the normal plane in the case when the core is located in the southern part of the area than in the case when the core is located in the northern part. If appropriate attenuation corrections are applied, then the densities reconstructed in the plane normal to the shower axis should be practically the same in both cases.

In order to reduce the effect of shower to shower fluctuations the same shower was used repeatedly, with the core positioned in a grid with the mesh size of 15 m, first in the northern part of the KASCADE-Grande area, then in the southern part. The energy deposition in the detectors was realistically simulated, then from the energy deposition the density was reconstructed using appropriate Lateral Energy Correction Functions. [16, 2]. The SHOWREC program [2] was used for analyzing the CORSIKA files, computing the energy deposition and obtaining the reconstructed density. The mesh size of 15 m assures that the same particles could not contribute to the signal of a given detector in more than one of the simulated showers.

Figures 15-20 show the densities obtained by using the orthogonal projection (Method 1) from the observation plane to the normal plane.

In Figure 15 the average density in the normal plane in the case when attenuation corrections are not applied is compared for 25 positions of the core in the northern part of the array to the average for 25 positions in the southern part of the array. Figure 15 presents
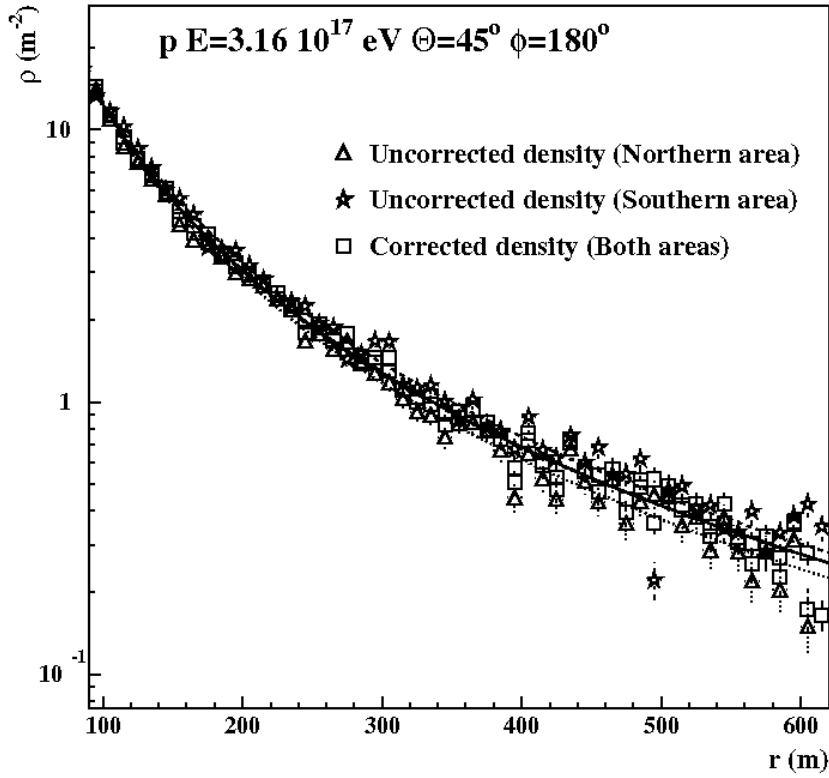
Figure 17: *Same as Fig. 15 for p induced showers.*

the case of the Fe induced shower, while Fig. 17 displays the same situation for the proton induced showers. The curves represent fits of the reconstructed densities using the Linsley lateral distribution function [17]. The density of case when the core is located in the southern part of the KASCADE-Grande array is indeed higher than in the case when the core is located in the northern part (see Figs.16 and 18 for the ratios of the densities). For example, in the case of Fe showers the density at 500 m for the showers with the core in the southern part of the array appears to be higher by 22% than the density in the same radial distance for the showers with the core located in the northern part. For proton showers, the result is roughly the same (23%). n view of a reconstruction of the primary energy by the S(500) observable [18] such a systematic bias is not negligible. Regarding the intensity integrated between 100 and 600 m the differences are in the order of 10% for the considered case. Figures 15 and 17 also display the densities which have been corrected for attenuation effects with the procedure presented in the previous chapters. The data obtained from both regions of the showers core were fitted again with the Linsley function and as expected, the results lie between the values obtained with uncorrected densities. It should be noted that in these cases applying the attenuation correction procedures to a given detector array, the values of r and cos Ψ are defined for each detector from the known arrival direction of the considered EAS.

The ability of the proposed correction procedure to remove the attenuation effects can be seen in Fig. 19 (the case of Fe induced showers) and 20 (the case of proton induced showers). There the corrected densities obtained in the average shower with the core located in the northern part and the corrected densities of the average shower with the core located in the southern part were independently fitted with Linsley functions. Obviously the attenuation correction procedure works efficiently.
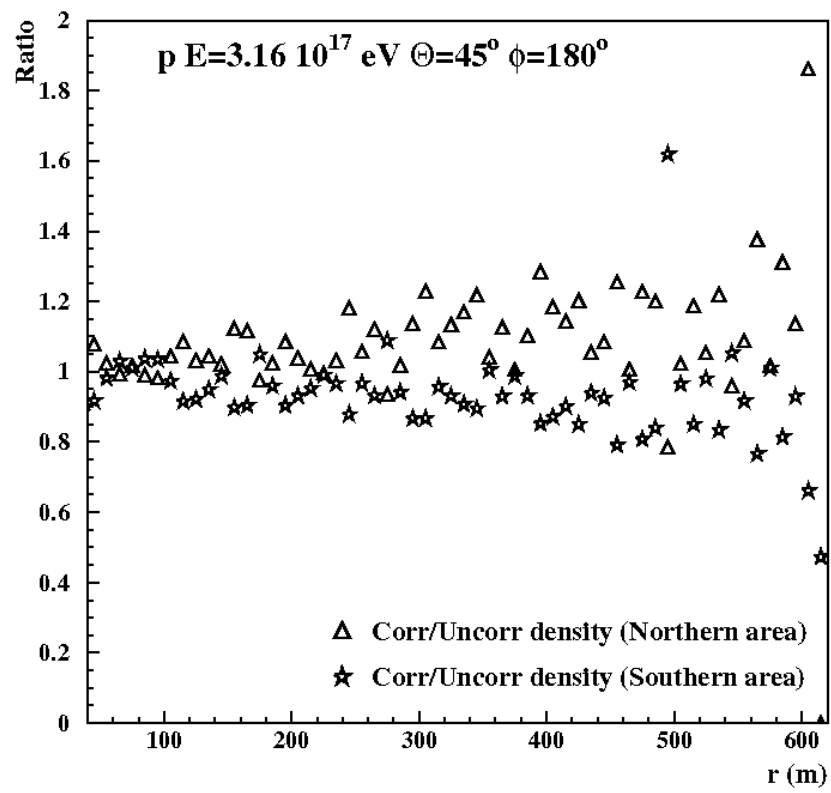
Figure 18: *The ratios of the corrected to the uncorrected densities (proton induced EAS)*
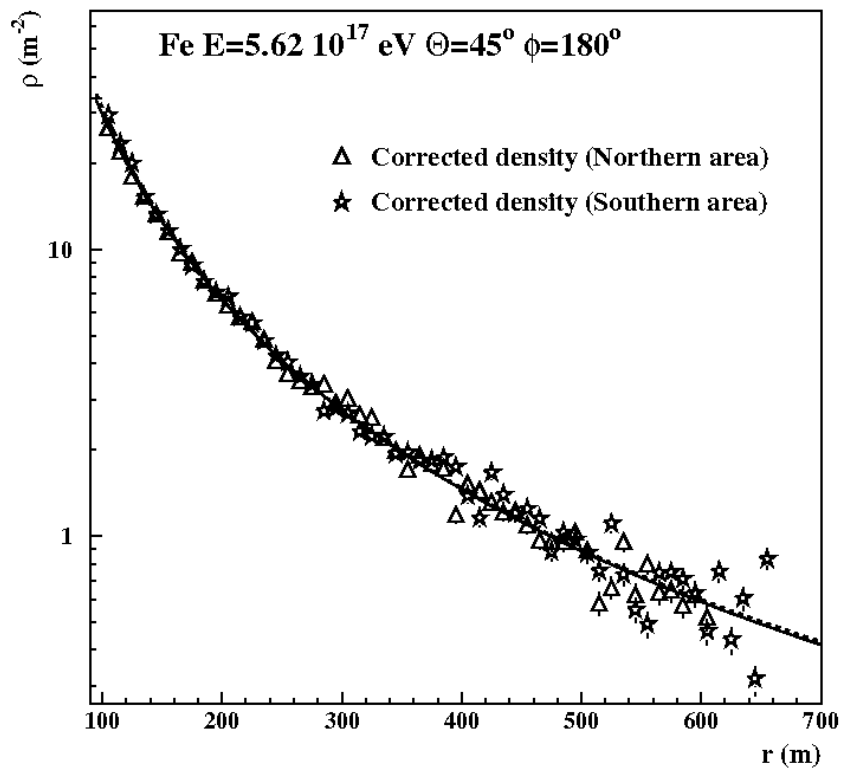
Figure 19: *Corrected lateral density distributions for Fe induced showers. Linsley fits of the density for showers with the core in the northern area (full line) and southern area (dashed line), respectively.18 The ratios of the corrected to the uncorrected densities (proton induced EAS)*
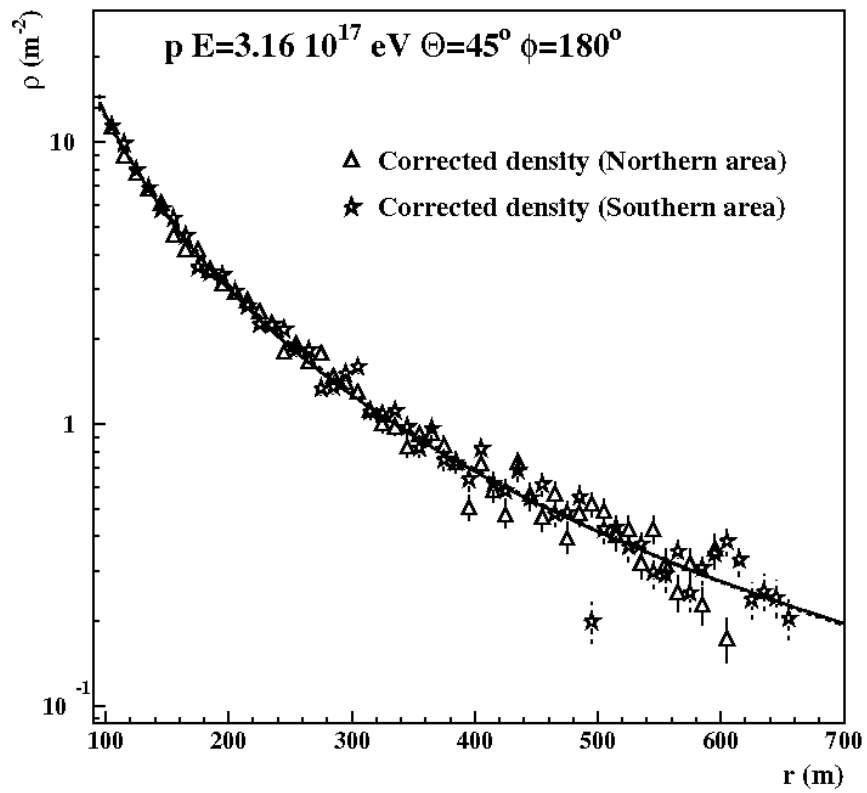
Figure 20: *Same as Fig. 19 for the case of p induced showers*

6 Concluding remarks

The lateral density distributions of charged EAS particles, reconstructed in the shower plane, display asymmetries and azimuthal variations in the case of inclined showers, even in the absence of the geomagnetic field. The origin of these asymmetries arise from the different attenuation of the particle density on different sides of the shower incidence, entangled with geometrical effects which are induced by the inaccuracies of the standard orthogonal projection from the observational plane to the shower plane. Accounting for these asymmetries is important, especially for quantities evaluated at large distances from the shower axis. An exponential correction function with attenuation coefficients depending mainly on the angle of incidence leads to reasonable good results, restoring the azimuthal symmetry. The inaccuracies resulting from the orthogonal projection, can be absorbed by a slight dependence of attenuation coefficient on the distance from the shower axis.

A corresponding correction procedure for the analysis of observed EAS has to include additionally the effects arising from the influence of the geomagnetic field on the lateral density distributions, based on the features worked out in refs.10-11. This work is in progress.

References

[1] A. Haungs, H. Rebel, M. Roth, Rep. Progr. Phys. 66 (2003) 1145

[2] O. Sima, I.M. Brancus, H. Rebel, A. Haungs, Report. FZKA 6985 Forschungszentrum Karlsruhe (2004); G.Toma et al. Proc. ECRS 2006, Lisbon, Portugal, so-134

[3] K. Kamata, J. Nishimura , Prog.Theor. Phys. 6 (suppl.) (1958) 93; K.Greisen, Ann. Rev. Nuc.Sci 10(1960) 63

[4] H. Rebel, O. Sima et al. KASCADE-Grande coll., Proc.29th ICRC 2005, Pune, India, Vol. 6, p.297

[5] X. Bertou, P. Billoir, Auger technical note Gap-2000-017 (2000) : www.auger.org

[6] A. Patrascioiu, O. Sima, H. Rebel, Internal Report KASCADE-Grande 2006-01; C. Morariu, C. Manailescu, O. Sima and H. Rebel, Internal Report KASCADE-Grande 2008-01

[7] C. Pryke, Pierre Auger technical note Gap-98-034 (1997) : www.auger.org

[8] M.T. Dova, L.N.Epele, A.G.Marazzi, Astropart.Phys. 18(2003)351

[9] A.M. Hillas et al., Proc 11th ICRC 1969, Budapest- Act Acad, Sci. Hungariae, Vol.29 (1970 suppl.), p.533

[10] H. Rebel, O. Sima, Romanian Rep. Phys.59(2007) 609; H. Rebel, O. Sima, A. Haungs, J. Oelschlaeger, Proc. 30th ICRC, Merida, Mexico, vol.5, p.1515

[11] H. Rebel et al., J.Phys G: Nucl. Part.Phys.35 (2008)085203

[12] D. Heck et al., Report FZKA6019, Forschungszentrum Karlsruhe (1998)

[13] A. Chiavassa et al., KASCADE-Grande coll., Proc.29th ICRC 2005, Pune, India, Vol. 6, p.313; G.Navarra et al.-KASCADE-Grande coll., Nucl.Instr.Meth.A518(2004) 207

[14] B.K. Xue and Bo-Qiang Ma, Astropart.Phys 27 (2007) 286

[15] O. Sima et al., Verhandlungen DPG (IV) 43, 2 (2008):*"The azimuthal asymmetry of particle lateral density in EAS in the range of observation of KASCADE-Grande"*, Freiburg i.Brsg 3. – 7. März 2008, contr. T 84.3

[16] C. Manailescu et al., Verhandlungen DPG (IV) 44, 2 (2009):„*Fast simulation of energy spectra of secondar EAS particles in Grande detectors and realistic computation of lateral correction Functions"*, München 9. – 13. März 2009, contr. T 98.2

[17] J. Linsley et al., Journ.Phys. Soc.Japan 17(1962)A-III

[18] G. Toma et al., KASCADE-Grande collaboration, Proc.30th ICRC, Merida, Mexico 2007, Vol. 4, p.227; G. Toma, PhD thesis, University of Bucharest, Romania, in preparation